Mode I strain energy release rate in composite laminates in the presence of voids

Mauro Ricotta, Marino Quaresimin, Ramesh Talreja

Mode I strain energy release rate in composite laminates in the presence of voids

Mauro Ricotta, Marino Quaresimin, Ramesh Talreja

PII: S0266-3538(08)00164-4
DOI: 10.1016/j.compscitech.2008.04.028
Reference: CSTE 4054

To appear in: *Composites Science and Technology*

Received Date: 26 February 2008
Accepted Date: 11 April 2008

Please cite this article as: Ricotta, M., Quaresimin, M., Talreja, R., Mode I strain energy release rate in composite laminates in the presence of voids, *Composites Science and Technology* (2008), doi: 10.1016/j.compscitech.2008.04.028

MODE I STRAIN ENERGY RELEASE RATE IN COMPOSITE LAMINATES IN THE PRESENCE OF VOIDS

Mauro Ricotta [a*], *Marino Quaresimin* [b], *and Ramesh Talreja* [c]

[a] Department of Mechanical Engineering, University of Padova, via Venezia,1 35131, Padova, Italy

[b] Department of Management and Engineering, University of Padova, stradella S. Nicola, 3 36100, Vicenza Italy

[c] Department of Aerospace Engineering, Texas A&M University, 736B H.R. Bright Building, College Station, Texas 77843-3141, USA

[*] Corresponding author, e-mail: mauro.ricotta@unipd.it

Abstract

The paper presents a methodology for evaluating the effects of voids on the fracture behaviour of woven fabric composites. The particular model studied consists of a double cantilever beam (DCB) in which voids are placed ahead of the crack tip and the Mode I Strain Energy Release Rate (SERR) is calculated. The standard beam-on-elastic-foundation theory is modified to account for shear compliance and material orthotropy, and the new formulation is used to evaluate the deformed shape, elastic deformation energy and SERR. The presence of the voids is simulated as an un-supported zone in the elastic foundation. The validation of the new analytical model, in terms of the deformed shapes and SERR values, is successfully carried out by suitable 2D Finite Element (FE) analyses. The effect of size, location and shape of the voids is investigated by a parametric study that showed that the enhancement of SERR increases with the size of the voids and the proximity to the crack tip and that elongated (elliptical) voids are more critical than the circular voids. Finally, the influence of more complex void distributions on the fracture toughness is evaluated by FE analysis.

Keywords: Strain Energy Release Rate, mode I, fracture, voids, woven.

1. INTRODUCTION

Voids are commonly found to form in composite manufacturing process and are likely to affect stiffness, strength and fracture properties. Since most of the cost of composite structures is often in the manufacturing process, it is important to assess the effect of voids in order to achieve cost-effectiveness. Voids can form by various reasons, e.g. by entrapment of air during liquid compression moulding and by enclosure of unfilled regions in resin transfer moulding. Inadequate temperature and pressure or tearing of the vacuum bag during the cure cycle can also contribute to their formation.

Significant efforts have been devoted to understanding of the void effects on composite mechanical properties. The results show that while the fibre dominated mechanical properties are not significantly influenced by voids [1,2,3,4], the matrix dominated properties are strongly dependent on their presence. Reduction in interlaminar shear [1,5,6], compressive [7,8], transverse [1,2], bending [1,3,9], fatigue [4,10,11,12] and fracture toughness [13,14,15] properties have been reported.

Wisnom et al. [5] investigated the influence of discrete and distributed voids on the interlaminar shear strength of glass/epoxy and carbon/epoxy UD laminates and reported a reduction ranging between 8 and 31% depending on the void size. Similar results were presented by Costa et al. [6] in the case of carbon/epoxy and carbon/bismaleimide fabric laminates. For the epoxy and bismaleimide resin the maximum reduction of the interlaminar shear strength was found to be 33% and 25%, respectively. SEM observations showed that the void location was strongly dependent on the matrix system. In the case of epoxy resin, in fact, the voids were preferentially located at the crossing of the woven fibre tows, while for carbon/BMI laminates the voids were found typically at interface of woven fibre tows. Moreover, observations carried out after interlaminar shear tests confirmed that in both cases the cracks nucleated from the voids, thus justifying the decrease in the interlaminar shear

strength. A similar decrease of ILSS was reported by Olivier et al. [1] by analysing the effects of cure cycle pressure on some mechanical properties of carbon/epoxy UD laminates. In the same paper the authors also investigated the void effects on tensile properties and they noticed that the longitudinal modulus as well as the longitudinal tensile strength (fibre-dominated properties) were not affected by voids. On the other hand, the transverse modulus and the transversal strength (matrix-dominated properties) were found to be extremely sensitive to the presence of defects with a reduction of 10 and 30%, respectively, for a void content of 10%. The shape and size of the voids also played an important role in the flexural behaviour. For a given void content, the specimens characterised by the largest voids showed a reduction in the bending modulus three times larger (15%) than those with small defects (5%).

Suarez et al. [7] investigated the effect of void content on the compressive strength of UD carbon/epoxy laminates. Their results indicate a roughly linear correlation between void content and compressive strength decrease, with a reduction of about 40% for 4% of void content. A reduced influence of voids was reported by Cinquin et al [8] for quasi isotropic carbon/epoxy laminates: in this case, the authors noticed a 14% reduction in the compressive strength for a void content of 11%.

Varna et al. [2] analysed the effect of voids on failure mechanisms in glass-fibre/vinylester fabric laminates produced by RTM and showed that increasing the void content decreased the transverse static strength. Results indicate an increase in the ultimate transverse strain to as high as 2% at high void content, whereas at low void content the laminates failed at 0.3%.

The influence of void content on flexural performance of UD glass fibre reinforced polypropylene composites was investigated by Hagstrand et al. [9]. Although they used different fibre and matrix with respect to reference [1], they found a decrease in both flexural modulus and bending strength of 20 and 28%, respectively, with a void content of 14%. Carbon/epoxy $[0/90]_{3s}$ laminates with different void contents have been investigated by Liu et

al. [3]. In order to correlate the void content with the mechanical properties, short beam shear, three-point bending and tensile tests were performed and significant reductions were found in interlaminar shear strength (the ILSS decreased by 6% for each 1% increase of voids), bending strength (the strength fell by 22% for a void content of 3.2%) and bending modulus (18% reduction for a void content of 3.2%).

The influence of void on fatigue behaviour is, in general, much more severe than the effect on the static properties. Almeida and Nogueira Neto [10] carried out four-point bending tests on $[0/90]_{12}$ carbon/epoxy laminates and found that a void content of 3% did not affect the static strength but had a detrimental effect on fatigue strength. Interesting results were reported by Bureau and Denault [4], for continuous glass fibre/polypropylene woven composites under cyclic bending: different void contents caused only a shift of the S-N curves without changing their slope, indicating a reduction of fatigue life with increasing voids. Tension-tension fatigue results for glass/epoxy $[0]_{10}$ fabric reinforced laminates, reported by Dill et al [11], indicate that fatigue strength reduction can be significantly greater than 20% for lower fatigue lives and close to 20% at lives of a few million cycles.

The damage evolution under flexural fatigue loading was investigated by Chambers et al. [12] for UD carbon fibre composites. They noticed that, by varying the void content from 1.6 to 3.1%, the fatigue life changed from 10^6 to 2000 cycles, under the same applied stress level. This detrimental effect was justified considering the fatigue damage evolution: the main damaging mechanism was a delamination located mainly in the mid-plane position. The authors asserted that the voids played a fundamental role in the fatigue life when they were detected in the inter-ply region where the delamination occurred.

The fracture toughness, measured as the critical Strain Energy Release Rate (SERR) value, was also found to be affected by the voids. Asp and Brandt [13] investigated the effects of pores and voids on the interlaminar delamination toughness of carbon/epoxy laminates,

carrying out static mode I, mode II and mixed mode ($G_{II}/G_I = 0.5$) tests. They found that the voids had deleterious or no effect on the critical SERR at crack growth initiation, depending on the irregularity of the void distribution. However, the void presence always increased the SERR values during propagation in mode I and in mixed mode. The authors attributed this behaviour to a change in failure mechanism: in the void-free specimens an insignificant amount of crack bridging was observed at the crack tip. In the coupons containing voids, however, ply splits were observed to bridge the crack. In the case of pure mode II loading, the effect of voids was always adverse. A very high sensitivity to voids for mode I fracture toughness was reported also by Olivier et al. [14]: a void content of 5% induces a decrease by about 22% in the mode I G_{IC}.

Rizov investigated the influence of void presence on the mode I fatigue behaviour of long glass reinforced injection moulded polypropylene plates [15]. An increase in the void content resulted in higher crack propagation rates. A limited influence was however reported for volume of voids lower than 1%, whereas higher contents (up to 7.14%) induced significant reductions in the crack propagation threshold and resistance.

On the basis of the extensive amount of experimental results available, initially some empirical approaches to correlate the material strength (interlaminar shear, bending, compressive and fatigue) with the void content were proposed. Only later, physics based models have been presented in the literature to assess the material response due to voids. For instance, starting from the experimental evidence, Almeida and Nogueira Neto [8] proposed a modified version of the Mar-Lin criterion [16] to evaluate both the static and fatigue behaviour of composite laminates under bending. Wisnom [5], proposed an analytical expression to predict the interlaminar shear strength starting from the Greszczuk's approach to evaluate the net section in the presence of void [17]. The ultimate tensile strain has been

studied by Varna [2], who proposed a simple model to explain the large strain to failure of high void content laminates.

Some analytical and computational models have also been proposed for predicting elastic properties in the presence of voids. A simple analytical approach, based on beam theory, was presented by Hagstrand [9] to evaluate the flexural modulus. A more complete and complex computational model was proposed by Huang and Talreja [18] who analysed the effects of void geometry on elastic properties of unidirectional laminates. Their model agreed with experimental data and predicted severe impact on the out-of-plane elastic properties due to voids. For example, for 6% voids of experimentally observed shape, they found reductions of 2% in longitudinal modulus E_x, 4% in transverse modulus E_y and 35% in the out of plane elastic modulus E_z. The authors noticed that, for a given void content, flat voids are benign for in-plane elastic properties but undesirable for out-of-plane stiffness. Long voids reduce the out-of-plane shear modulus significantly, but have little effect on the in-plane properties.

In the literature some analytical approaches are available for evaluating the fracture toughness of composite laminates, but only in the absence of voids.

One of the first models was proposed by Kanninen [19], who studied the influence of the region beyond the crack tip on SERR, by developing a model based on the theory of beams on elastic foundation. One of the aims of the paper was to evaluate the Mode I SERR G_I, and the Stress Intensity Factor K_I, on a DCB specimen, accounting for the influence of length and height of the specimen, in order to study both the initial crack extension and the unstable crack propagation. The main result presented in [19] is that, for calculating K_I (and G_I), the simple built-in beam model is applicable only when both the specimen length beyond the crack tip and the initial crack length are very large compared to the beam height, otherwise one must account for the effect of the region beyond the crack tip.

Suo et al. [20] presented an interesting approach to analyse the role of material orthotropy on G_I, called orthotropy rescaling technique, which can reduce plane elastic problems for orthotropic materials to equivalent ones for materials with cubic symmetry. This method is based on two dimensionless parameters, based on the elastic properties of the material, and on the solution of the local equilibrium equations by means of a dedicated Airy stress function. The orthotropy rescaling technique allowed the authors to extract approximate solutions for orthotropic materials on the basis of known isotropic solutions, such as those of stress intensity factors and stress concentration factors.

Williams et al. in [21] analysed the influence of the shear on Mode I SERR considering the DCB geometry. Starting from the integration of the local equilibrium equations, they proposed an analytical solution to evaluate G_I, which includes two constants to be calculated by FE analyses.

The methods discussed above and others reported in the literature provide means for evaluating the SERR in composite cracked beams. However, it seems that analytical tools describing the crack-void interaction are available only for isotropic plate loaded in tension (see [22-25] for some examples) and, to the best of authors' knowledge, no solutions have been developed so far for composite DCBs.

In an attempt to provide a contribution in this area, the paper presents an analytical model suitable to describe the SERR in a DCB under mode I loading in the presence of voids. The model is based on the beam-on-elastic-foundation theory refined to include the shear effect. The presence of voids is simulated by an unsupported zone in the elastic foundation. After presentating the analytical framework of a refined beam theory, developed to account for the transverse shear compliance, the mode I SERR component is analytically evaluated following Kanninen's approach [19] and the shear effect is analysed. Then, the analytical model is extended to include the presence of voids and the influences of their shape, dimension and

position are investigated. The analytical approach is validated by comparison with the results obtained by dedicated Finite Element analyses, performed by using the Virtual Crack Closure Technique (VCCT) [26,27]. Finally, FE analyses are used to analyse more complex void distributions.

2. REFINED BEAM THEORY INCLUDING SHEAR EFFECT

The proposed model is based on the beam on elastic foundation approach, including shear effect and material orthotropy. The analytical background is described below, considering the co-ordinate system shown in figure 1.

For an elastic body undergoing small displacements, the strain-displacement equations are:

$$\varepsilon_x = \frac{du}{dx} \qquad \varepsilon_z = \frac{dw}{dz} \qquad \varepsilon_{xz} = \frac{1}{2}\left(\frac{du}{dz} + \frac{dw}{dx}\right) \tag{1}$$

where *u* and *w* are the displacements in the x and z directions, respectively, and their functional forms can be written as:

$$\begin{aligned} u(x,z) &= u_0(x) + z \cdot \theta(x) \\ w(x) &= w(x) \end{aligned} \tag{2}$$

where u_0 is the midplane displacement in the x-direction.

In classical beam theory θ(x) is the negative of the first derivative of the lateral displacement w with respect to x. However, if transverse shear compliance is non zero, θ(x) is an unknown dependent variable which must be determined. Therefore, to include shear deformation effect, one uses the third of (1).

Now, substituting the admissible form of the displacement into third of (1), we have

$$\varepsilon_{xz} = \frac{1}{2}\left(\theta(x) + \frac{dw}{dx}\right) \tag{3}$$

To determine the resulting three geometric unknowns, $u_0(x)$, $w(x)$ and $\theta(x)$, it is necessary to consider the equilibrium, constitutive and compatibility equations, as well as the strain-displacement relationships.

For a midplane symmetric beam made of orthotropic material (without coupling terms), the constitutive equations are:

$$N_x = A_{11}\varepsilon_x^0 = \left[\frac{E_x}{(1-\nu_{xy}\cdot\nu_{yx})}\cdot h\right]\cdot\varepsilon_x^0 \tag{4}$$

$$Q_x = 2A_{55}\varepsilon_{xz} = 2\left(\frac{G_{xz}\cdot h}{\chi}\right)\cdot\varepsilon_{xz} \tag{5}$$

$$M_x = D_{11}\frac{d\theta(x)}{dx} = \left[\frac{E_x}{(1-\nu_{xy}\cdot\nu_{yx})}\cdot\frac{h^3}{12}\right]\cdot\frac{d\theta(x)}{dx} \tag{6}$$

where N_x and Q_x are the normal and shear stress resultants and M_x is the stress couple per unit edge distance; ε_x^0 is the middle surface strain in x direction; A_{11}, A_{55} and D_{11} are the terms of stiffness matrix derived from the lamination theory, E_x is the Young modulus in x direction, ν_{xy} and ν_{yx} are the Poisson's coefficients, G_{xz} is the shear modulus, h is the beam height and and χ is the shear factor (figure 1). The equilibrium of the beam can be written as:

$$\frac{dQ_x}{dx} + p(x) = 0 \tag{7}$$

$$\frac{dM_x}{dx} - Q_x = 0 \tag{8}$$

where p(x) is the lateral load acting in the z-direction.

The elastic foundation is usually described in the literature as an elastic medium with a constant foundation modulus. This foundation, represented by a spring bed, acts on the beam

as a distributed load, proportional to the local lateral displacement w(x). The force per unit area p(x) is therefore –k·w(x) and the equation (7) becomes:

$$\frac{dQ_x}{dx} - k \cdot w(x) = 0 \tag{9}$$

Substituting (3) into (5), through (7) and (8), it is possible to write the following ordinary differential equation (ODE) system as

$$\begin{cases} \dfrac{d^3\theta(x)}{dx^3} = \dfrac{12 \cdot (1 - \nu_{xy} \cdot \nu_{yx})}{E_x \cdot h^3} k \cdot w(x) \\ \dfrac{d\theta(x)}{dx} + \dfrac{d^2 w(x)}{dx^2} = \dfrac{\chi}{G_{xz} \cdot h} k \cdot w(x) \end{cases} \tag{10}$$

After double differentiation of the last equation, we obtain:

$$\frac{d^3\theta(x)}{dx^3} = -\frac{d^4 w(x)}{dx} + \frac{d^2 w(x)}{dx^2} \frac{\chi \cdot k}{G_{xz} \cdot h} \tag{11}$$

and substituting the first of Eq. (10), we obtain the governing fifth order ODE system for a beam on elastic foundation including the shear effect, as

$$\begin{cases} \dfrac{d^3\theta(x)}{dx^3} = \beta \cdot w(x) \\ \dfrac{d^4 w(x)}{dx} - \alpha \dfrac{d^2 w(x)}{dx^2} + \beta \cdot w(x) = 0 \end{cases} \tag{12}$$

where $\alpha = \dfrac{\chi \cdot k}{G_{xz} \cdot h}$ and $\beta = \dfrac{12 \cdot (1 - \nu_{xy} \cdot \nu_{yx}) \cdot k}{E_x \cdot h^3}$

The integration of last equation of (12) gives the w(x) expression and then from the first equation we can obtain θ(x). The general solution for w(x) is:

$$w(x) = \sum_{i=1}^{4} c_i e^{\lambda_i x} \tag{13}$$

where λ_i are the roots of the characteristic polynomial and c_i constants depending on boundary conditions. The λ_i are:

$$\lambda_{1,2} = \pm\frac{1}{2}\sqrt{2\alpha + \sqrt{2\left(\alpha^2 - 4\beta\right)}}; \quad \lambda_{3,4} = \pm\frac{1}{2}\sqrt{2\alpha - \sqrt{2\left(\alpha^2 - 4\beta\right)}} \tag{14}$$

and they can be either real or complex depending on the elastic material constants. Considering that $\lambda_2 = -\lambda_1 = \delta$ and $\lambda_4 = -\lambda_3 = \varepsilon$, the displacement w(x) becomes

$$w(x) = c_1 e^{\delta x} + c_2 e^{-\delta x} + c_3 e^{\varepsilon x} + c_4 e^{-\varepsilon x} \tag{15}$$

Hence, the equation of the beam curvature is

$$\theta(x) = c_1 e^{\delta x}\left(\frac{\alpha - \delta^2}{\delta}\right) - c_2 e^{-\delta x}\left(\frac{\alpha - \delta^2}{\delta}\right) + c_3 e^{\varepsilon x}\left(\frac{\alpha - \varepsilon^2}{\varepsilon}\right) - c_4 e^{-\varepsilon x}\left(\frac{\alpha - \varepsilon^2}{\varepsilon}\right) + c_5 \tag{16}$$

The constant c_5 must be zero to satisfy (8) for each value of the co-ordinate x.

When G_{xz} tends to infinity, the last equation of system (12) becomes the classical fourth order differential equation of beam on elastic foundation reported in Ref. [19].

3. MODE I STRAIN ENERGY RELEASE RATE

The Mode I fracture toughness in composite laminates is usually measured on DCB specimens. In the DCB analysis, one can take advantage of the geometric symmetry and model only half of the specimen, as frequently done in literature. The support provided by the remaining part is represented by an elastic foundation with stiffness depending on the material properties. Following Kanninen's approach [19] and using the new formulation described above, the mathematical description of a DCB arm can be made by considering two geometry

domains (-a,0) and (0,c) separately and then matching the values of w(x) and θ(x) and the equilibrium equations at x=0, (see figure 2). Furthermore, at x=c, both bending moment and shear force must be zero; at x=-a shear force must be -F and bending moment zero. Considering the material orthotropy and according to ref. [19], the value of spring bed stiffness can be calculated as $k = 2b \cdot E_{zz}/h$. For $-a \le x \le 0$ the parameter k becomes, obviously, zero and the solutions of system (12) are polynomial functions.

The results obtained from the analytical model for w(x) and θ(x), considering the material properties, geometry and load data listed in Table 1, are plotted in figure 3. The results of the FE validation discussed later are also reported in the figure.

Once the displacement function is known, the elastic strain energy W of the beam shown in figure 2 can be evaluated as the external work done by the applied load F per unit width. Considering that the DCB specimen is characterised by two arms, the elastic strain energy W of the entire specimen is:

$$W = 2 \cdot \frac{1}{2} F \cdot w(x = -a) \tag{17}$$

Hence, the Mode I component of SERR is:

$$G_I = \frac{dW}{da} = \frac{\partial W}{\partial a} - \frac{\partial W}{\partial c} \tag{18}$$

The closed form for G_I was obtained by using the symbolic toolbox of Matlab 6.5 code. The proposed analytical model allows the influence of the shear modulus G_{xz} on G_I to be evaluated. Figure 4 shows the results obtained with the data summarised in Table 1: as expected, an increase in the transverse shear modulus G_{xz} induces a decrease in the Mode I SERR. In the same figure, the G_I values calculated following the classical beam theory and Kanninen's approach are reported. The error ranges from 30.6 to 13.8% and from 25.2 to

7.0%, respectively, for the two approaches, with increasing value of the shear modulus. FE results are also reported for comparison.

4. EFFECT OF VOIDS ON STRAIN ENERGY RELEASE RATE

The analytical model described above can now be effectively applied to investigate the potential effects of voids on the Mode I component of SERR. The application is restricted here to the case of a single void, since the extension to the case of multiple aligned voids is conceptually straightforward and characterised only by a significant increase of mathematical formalism. To describe the void presence beyond the crack tip, the beam length for $0 \le x \le c$ is divided into three separate zones: the first and the third on elastic foundation and the second, simulating the void, without constraints and characterised by suitable moment of inertia J_v and area A_v (see figure 5).

Considering the integral average of the beam height evaluated in the void region, J_v and A_v were calculated through the following equations:

$$J_v = \frac{b}{12}\frac{1}{2R}\int_{-R}^{R}\left(h-\sqrt{R^2-x^2}\right)^3 dx = \frac{b}{12}\left(h-\frac{\pi\cdot R}{4}\right)^3 \tag{19}$$

$$A_v = b\frac{1}{2R}\int_{-R}^{R}\left(h-\sqrt{R^2-x^2}\right)dx = b\left(h-\frac{\pi\cdot R}{4}\right) \tag{20}$$

Then, the first and the third domains are described by an ODE system in the following form:

$$\begin{cases} \dfrac{d^3\theta(x)}{dx^3} = \beta\cdot w(x) \\ \dfrac{d^4w(x)}{dx} - \alpha\dfrac{d^2w(x)}{dx^2} + \beta\cdot w(x) = 0 \end{cases} \qquad \begin{matrix} 0 \le x \le d-R \\ d+R \le x \le c \end{matrix} \tag{21}$$

where "d" is the distance between the crack tip and the centre of the void and “R” is the void radius.

On the other hand, the "unsupported" domains are described by:

$$\begin{cases} \dfrac{d^3\theta(x)}{dx^3} = 0 & -a \le x \le 0 \quad (J, A) \\ \dfrac{d\theta(x)}{dx} + \dfrac{d^2w(x)}{dx^2} = 0 & d-R \le x \le d+R \quad (J_V, A_V) \end{cases} \tag{22}$$

A similar approach can be used in the case of a single elliptical void, with maximum and minimum axes of length 2e and 2f, respectively. J_v and A_v are evaluated by substituting "f" for "R" in equations (19) and (20) and the domain of integration is defined by considering "e" for "R" in equations (21) and (22). The deformed state of the specimen is then described by four fifth order ODE systems, which require 20 constants to be determined for the solution. The equilibrium and compatibility equations used are summarised in Table 2. As a further condition, the solution of each ODE system must again satisfy the equilibrium equation (8).

The previous conditions generate a linear system of 20 equations, which was solved by using the symbolic toolbox of Matlab 6.5 code. After the calculation of the work done by the external loads, the Mode I SERR can be evaluated as:

$$G_{I,v} = \frac{dW_v}{da} = \frac{\partial W_v}{\partial a} - \frac{\partial W_v}{\partial d} - \frac{\partial W_v}{\partial c} \tag{23}$$

Some results of the application of the new model are presented in figures 6-8. In figure 6, the effect of a void is represented by the ratio between the SERR evaluated in the presence of the void, $G_{I,V}$, and the SERR for the pristine specimen G_I. The analysis was made for both circular and elliptical voids, at several distances between void and crack tip. Figure 7 shows the effect of the void size and it is clearly evident that the SERR values increase in the presence of larger voids located in the vicinity of the crack tip. The shape of the elliptical voids was also found to have a significant effect, with elongated voids being much more critical (figure 8).

5. MODEL VALIDATION

The validation of the analytical model was done by a comparison with the results obtained by dedicated FE analyses. A 2D FE model was developed by using the Ansys 8.0® code and PLANE82 elements under plane strain conditions. Material properties, geometry and load data are listed in Table 1.

As first check, the results obtained from the analytical model for w(x) and θ(x) were compared (see figure 3). It is important to highlight that the comparison is made between a 1D (analytical) model with a 2D (FE) model. For this reason, during the FE analyses, the w(x) and θ(x) values were evaluated on both middle and top surfaces of the arm. A general good agreement between analytical and numerical results can be observed in figure 3, confirming the accuracy of the analytical model proposed above. However, in the $0 \le x \le c$ domain (figure 3b), significant discrepancies between analytical and FE middle surface solution for w(x) and analytical and FE top surface solution for θ(x) were found. This apparent inconsistency can be easily justified when considering the dimensionality of the problem (1D for the analytical model, 2D for the FE model).

As a further validation of the analytical model, the influence of the transverse shear modulus G_{xz} on the Mode I component of SERR is calculated and compared with suitable FE calculations (see figure 4). The FE evaluation of G_I was made by applying the VCCT [26, 27]. As required by this method, the region near the crack tip was modelled with regular shape elements of uniform size, as shown in figure 9. The element size "e" was chosen equal to 0.005 mm for the DCB model without voids. In the case of void presence, instead, the "e" value was imposed equal to 1/20 of the void radius R.

As shown in figure 4, where the influence of shear modulus on G_I is analysed, a good agreement between analytical and numerical results was found (maximum error around 4%).

In order to validate the present analytical model in the case of voids, several FE analyses were performed to calculate the mode I SERR component for different dimensions, shape and distribution of voids from the crack tip. As shown in figure 6, the analytical results obtained from Eq. (23) are in reasonably good agreement with FE calculations.

5.1 Multiple aligned voids

As previously described, the proposed analytical model can be extended in the case of multiple aligned voids with a significant increase in the mathematical formalism. Only for this reason we decided to investigate the influence of multiple voids on G_I by means of 2D FE analyses. Again the VCCT method was used and 2 and 3 aligned circular voids were considered, changing both the distance from the crack tip "d" and the mutual distance "D" between the voids, as shown in figure 10.

In figure 11 are shown the FE results obtained in the case of multiple aligned circular voids, with a radius of 0.1 mm and mutual distance kept constant and equal to 2 mm. The influence on G_I here is similar to that for the single void, but the influence is greater. Moreover, increasing the number of aligned voids, it seems that the influence on mode I of SERR is controlled by the first 2 voids.

When the position of the first void is fixed, as shown in figure 12, the effect of voids beyond the nearest one from the crack tip shows a maximum at a characteristic distance from the first void.

6. CONCLUSIONS

A new methodology for the evaluation of Mode I Strain Energy Release Rate for composite DCB specimens in the presence of voids has been presented and discussed.

The analytical model is based on the beam-on-elastic foundation theory, improved and modified to account for transverse shear effect and material orthotropy. The presence of a single void in front of the crack tip has been considered here; the extension to the case of more aligned voids requires only a significant increase in the mathematical formalism without any conceptual difficulty. After a successful validation based on FE analyses, the application of the model allowed us to investigate the influence on the SERR of design parameters like material properties, location, shape and size of the void. Finally, different void distributions were analysed, in order to investigate the influence of other parameters such as the number of the voids aligned behind the crack tip and their mutual distance.

The main results can be briefly summarised as follows:

- the Mode I SERR in DCB specimens is significantly influenced by the transverse shear properties of the laminate;
- in the presence of voids, SERR values increase as the dimension of the void increases and with the decrease in the distance between void and crack tip;
- the void shape plays an important role: circular and elliptical voids are equally critical when they have the same longitudinal size (R=e). On the other hand, elliptical voids are much more critical when the vertical size is the same (R=f). Morever, SERR values for elliptical void increase significantly with the aspect ratio.
- with increasing number of aligned voids it seems that the influence on G_I is controlled by the first two voids.
- the effect of voids beyond the nearest one from the crack tip shows a maximum at a characteristic distance from the first void.

Finally, considering the results presented in this paper, a general conclusion can be drawn. Even supported by the experimental observations presented by Asp [13], in the authors' opinion the presence of voids cannot be measured by using only their volume content. In fact

important parameters are their position, shape and dimensions. For the effect of voids on fracture toughness, a small void near the crack tip has a stronger influence than a big void far away from the crack tip.

REFERENCES

1. Olivier, P., Cottu, J.P., Ferret, B., "Effects of cure cycle pressure and voids on some mechanical properties of carbon/epoxy laminates", *Composites*, 26, 1995, 509-515.
2. Varna, J., Joffe, R., Berglund, L.A. and Lundström, T.S., "Effect of voids on failure mechanisms in RTM laminates", *Compos Sci Technol*, 53, 1995, 241-249.
3. Ling Liu, Bo-Ming Zhang, Dian-Fu Wang, Zhang-Jun Wu, "Effects of cure cycles on void content and mechanical properties of composite laminates", *Compos Struct*, 73, 2006, 303-309.
4. Bureau, M.N., Denault, J., "Fatigue resistance of continuous glass fiber/polypropylene composites: consolidation dependence", *Compos Sci Technol*, 64, 2004, 1785-1794.
5. Wisnom, M.R., Reynolds, T., Gwilliam, N., "Reduction in interlaminar shear strength by discrete and distributed voids", *Compos Sci Technol*, 56, 1996, 93-101.
6. Costa, M.L., Almeida, S.F.M, Rezende, M.C., "The influence of porosity on the interlaminar shear strength of carbon/epoxy and carbon/bismaleimide fabric laminates", *Compos Sci Technol* 61, 2001, pp. 2101-2108.
7. Suarez, JC., Molleda, F., Güemes, A., "Void content in carbon fiber/epoxy resin composites and its effects on compressive properties", *Proceedings of ICCM-9*, Spain, Woodhead Publishing Limited, 1993, pp. 589-596.
8. Cinquin, J., Triquenaux, V. and Rousne, Y., "Porosity influence on organic composite material mechanical properties", Proc. of ICCM 16, 16th International Conference on Composite Materials, 8th-13th July 2007, Kyoto, Japan.
9. Hagstrand, P.-O., Bonjour, F. Månson, J.-A.E., "The influence of void content on the structural flexural performance of unidirectional glass fibre reinforced polyprolylene composites", *Compos Part A-Appl S*, 36, 2005, 705-714.

10. Almeida SFM, Nogueira Neto ZS, "Effect of void content on the strength of composite laminates", *Compos Struct*, 28, 1994, 139-148.
11. Dill, C.W., Tipton, S.M., Glaessgen, E.H. and Brasnscum, K.D., "Fatigue strength reduction imposed by porosity in a fiberglass composite", Damage Detection in Composite Materials, ASTM STP 1128, J.E. Masters, Ed., American Society for Testing and Materials, 1992, pp. 152-162.
12. Chambers, A.R., Earl, J.S., Squires, C.A., Suhot, M.A., "The effect of voids on the flexural fatigue performance of unidirectional carbon fibre composites developed for wind turbine applications", *Int J Fatigue*, 28, 2006, pp. 1389-1398.
13. Asp, Leif E. and Brandt, F., "Effects of pores and voids on the interlaminar delamination toughness of a carbon/epoxy composite", Proc. of ICCM-11, Goald Coast, Australia, 14th-18th July 1997.
14. Olivier, P. A., Mascaro, B., Margueres, P., Collombet, F., "CFRP with voids: ultrasonic characterization of localized porosity, acceptance criteria and mechanical characteristics", Proc. of ICCM 16, 16th International Conference on Composite Materials, 8th-13th July 2007, Kyoto, Japan.
15. Rizov, V.I., "Voids and their effects on the fatigue fracture behavior of long glass fibre reinforced injection molded polypropylene", Proc. of ECCM12, 12th European Conference on Composite Materials, August 29-september 2, 2006, Biarritz, France.
16. Mar, J.W., Lin, K.Y., "Fracture correlation for tensile failure of filamentary composites with holes", *J Aircraft*, 14, 1977, 703-704.
17. Greszczuk, L.B., "Effect of voids on strength properties of filamentary composites", *22nd Annual Meeting of the Reinforced Plastic Division*, Society of the Plastics Industry, Washington DC, 1967, 20A1-20A10.

18. Huang, H., Talreja, R., "Effects of void geometry on elastic properties of unidirectional reinforced composites", *Compos Sci Technol*, 65, 2005, 1964-1981.

19. Kanninen, M.F., "An augmented double cantilever beam model for studying crack propagation and arrest", *Int J Fracture*, 9, 1973, pp.83-92.

20. Suo, Z., Bao, G., Fan, B., and Wang, T.C, "Orthotropy rescaling and implications for fracture in composites ", *Int J Solids Struct,* 28, 1991, pp. 235-248.

21. Williams, J.G., Hadavinia, H., Cotterell, B., "Anisotropic elastic-plastic bending solutions for edge constrained beams", *Int J Solids Struct,* 42, 2005, pp. 4927-4946.

22. Isida, M., "On the determination on stress intensity factors for some common structural problem", *Eng Fract Mech*, 1970, 2, pp 61-79.

23. Isida, M., Chen, D.H., Nisitani, H., "Plane problems of an arbitrary array of crack emanating from the edge of an elliptical hole, *Eng. Fract. Mech.*, 1985, 21, pp. 983–995.

24. Erdogan, F., Gupta, G.D., Ratwani, M.,"Interaction between a circular inclusion and an arbitrarily oriented crack", *J Appl Mech,* 1974, pp.1007-1011.

25. X. Hu, A. Chandra and Y. Huang "Multiple void-crack interaction" *Int J Solids Struct,* 1993, Volume 30, Issue 11, pp. 1473-1489.

26. Rybicki, E. F. and Kanninem, M. F., “A finite element calculation of stress intensity factors by a modified crack closure integral”**,** *Eng Fract Mech*, **9** (1977), 931-938.

27. Raju, I. S., “Calculation of strain energy release rates with higher order and singular finite elements”, *Eng Fract Mech*, 28/3 (1987), 251-274.

List of captions to figures and tables

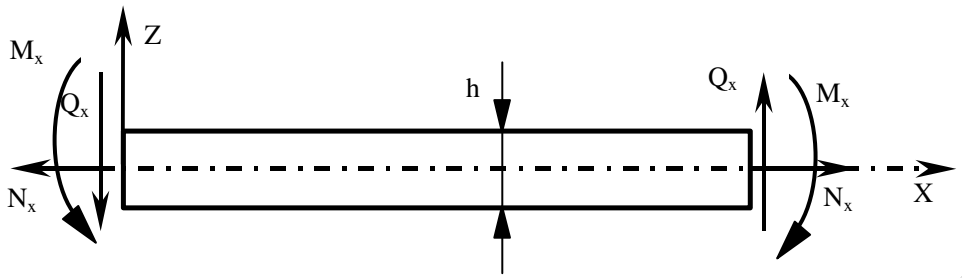

Figure 1: Co-ordinate system and positive directions for stress resultants and stress couple (per unit edge length in the y-direction)

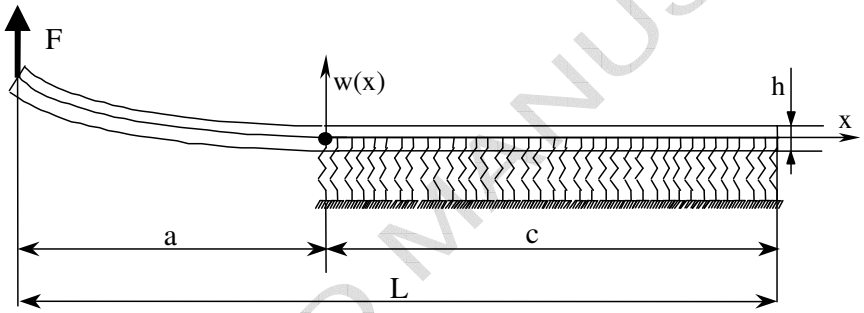

Figure 2. Beam-on-elastic-foundation model of one arm of a DCB specimen

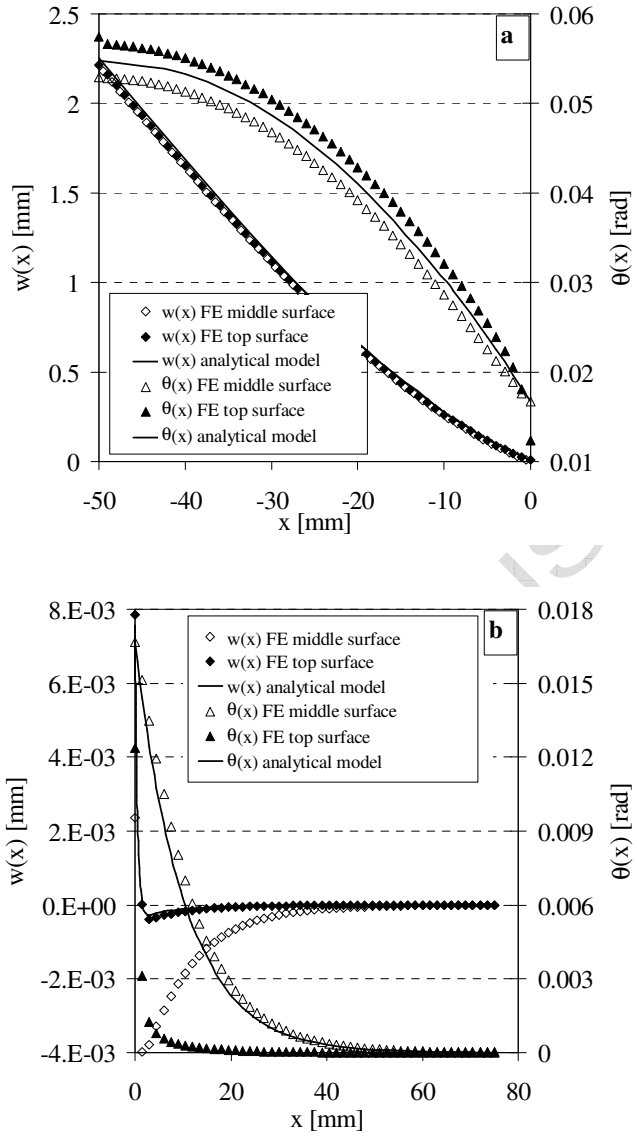

Figure 3. Comparison between analytical model and FE results

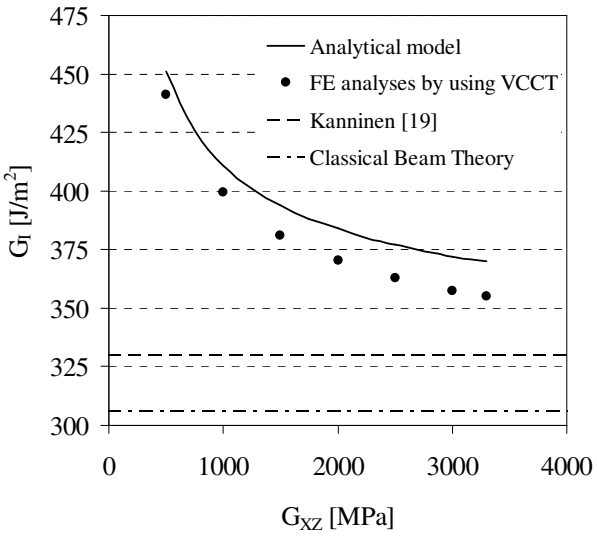

Figure 4. Influence of shear modulus G_{xz} on Mode I component of SERR.

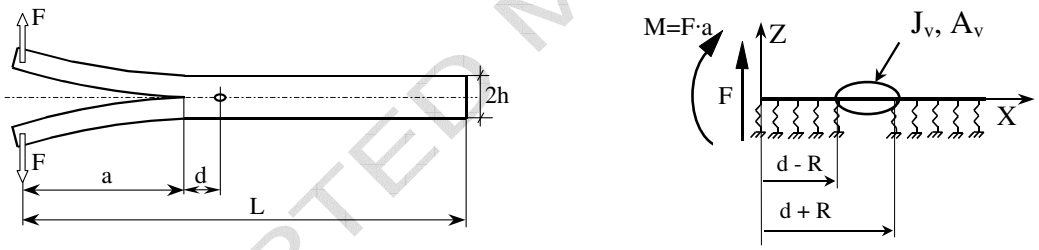

Figure 5. Model of void presence based on the beam-on-elastic-foundation approach.

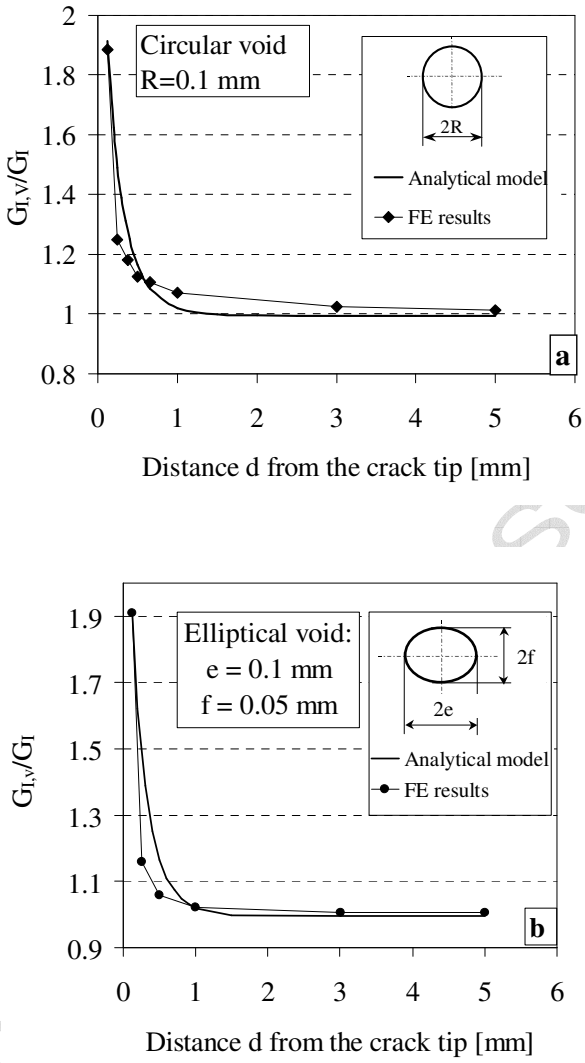

Figure 6. Effect of the void presence on the Mode I component of SERR

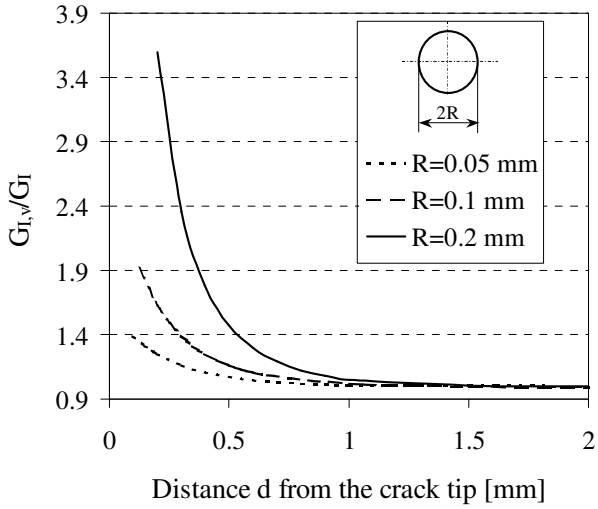

Figure 7. Influence of the void size

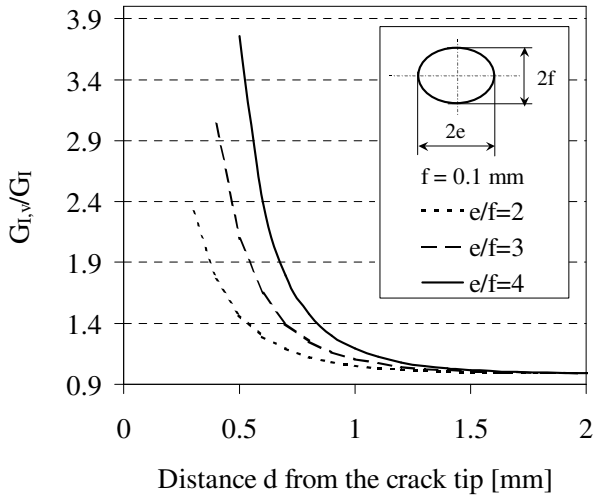

Figure 8. Influence of aspect ratio for elliptical void

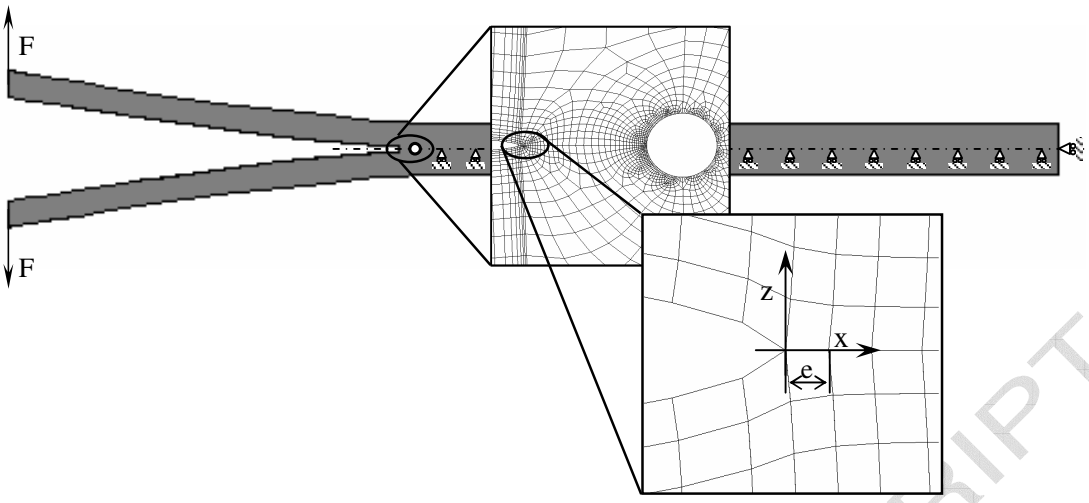

Figure 9. Finite element model of the DCB with boundary conditions and details of the mesh near the crack tip and around the void edge.

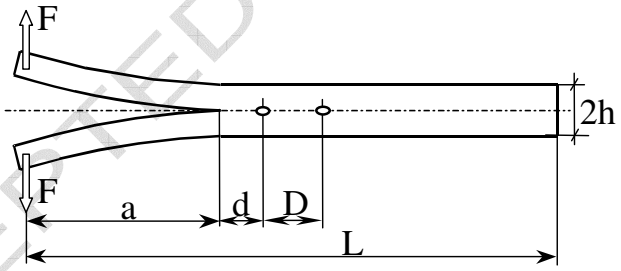

Figure 10. Schematic view of the analysed parameters in the case of multiple aligned voids.

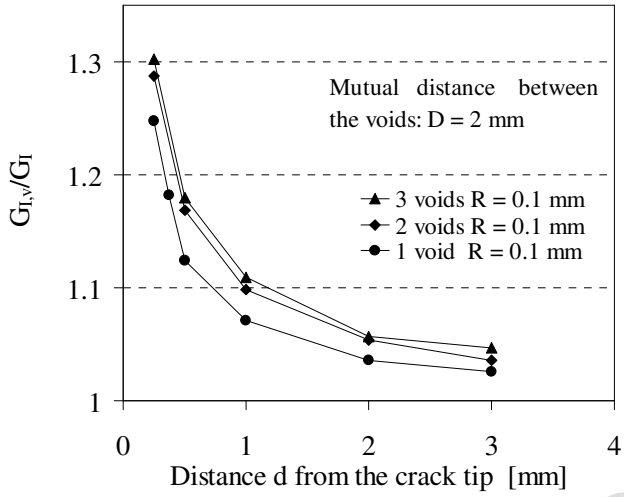

Figure 11. Influence of the number of the voids on G_I.

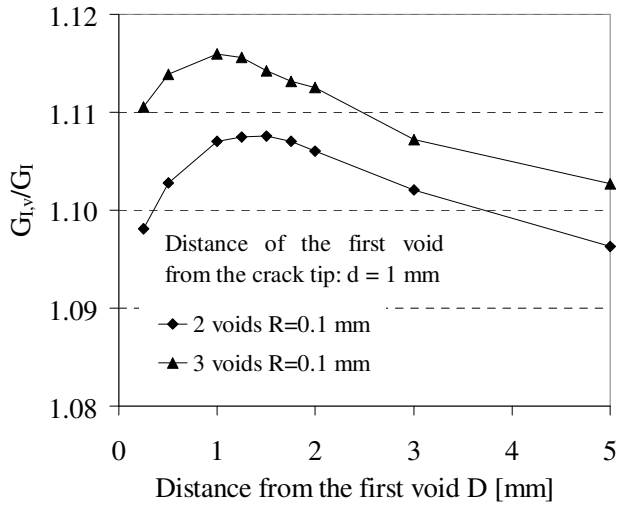

Figure 12. Effect on G_I of the number of aligned voids with different mutual distances.

Table 1: Elastic material properties, DCB geometry and external applied load.

E_x [MPa]	E_y [MPa]	E_z [MPa]	G_{xz} [MPa]	G_{xy} [MPa]	ν_{xy}	$\nu_{xz,}$ ν_{yz}	h [mm]	b [mm]	a [mm]	c [mm]	F [N]
58050	58050	6500	500	3300	0.06	0.3	3	25	50	75	100

Table 2: Equilibrium and compatibility equations in the case of a single void

x = -a	x = 0	x = d-R
$M_x = 0$ $Q_x = -F$	$(M_x)_{x=0^-} = (M_x)_{x=0^+}$ $(Q_x)_{x=0^-} = (Q_x)_{x=0^+}$ $(w)_{x=0^-} = (w)_{x=0^+}$ $(\theta)_{x=0^-} = (\theta)_{x=0^+}$	$(M_x)_{x=(d-R)^-} = (M_x)_{x=(d-R)^+}$ $(Q_x)_{x=(d-R)^-} = (Q_x)_{x=(d-R)^+}$ $(w)_{x=(d-R)^-} = (w)_{x=(d-R)^+}$ $(\theta)_{x=(d-R)^-} = (\theta)_{x=(d-R)^+}$
	x = d+R	x = c
	$(M_x)_{x=(d+R)^-} = (M_x)_{x=(d+R)^+}$ $(Q_x)_{x=(d+R)^-} = (Q_x)_{x=(d+R)^+}$ $(w)_{x=(d+R)^-} = (w)_{x=(d+R)^+}$ $(\theta)_{x=(d+R)^-} = (\theta)_{x=(d+R)^+}$	$M_x = 0$ $Q_x = 0$